

TRPV1 Gates Tissue Access and Sustains Pathogenicity in Autoimmune Encephalitis

Geoffrey Paltser,^{1,2*} Xue Jun Liu,^{1,3*} Jason Yantha,^{1,2} Shawn Winer,^{1,2} Hubert Tsui,^{1,2} Ping Wu,^{1,2} Yuko Maezawa,^{1,2} Lindsay S Cahill,⁴ Christine L Laliberté,⁴ Sreeram V Ramagopalan,⁵ Gabriele C DeLuca,⁵ A Dessa Sadovnick,⁶ Igor Astsaturov,⁷ George C Ebers,⁵ R Mark Henkelman,⁴ Michael W Salter,^{1,3} and H-Michael Dosch^{1,2}

¹Neuroscience and Mental Health Program, Research Institute, The Hospital for Sick Children, Toronto, Ontario, Canada, ²University of Toronto, Departments of Immunology and Pediatrics, Toronto, Ontario, Canada, ³University of Toronto, Department of Physiology, Toronto, Ontario, Canada, ⁴Mouse Imaging Centre, The Hospital for Sick Children, Toronto, Ontario, Canada, ⁵Wellcome Trust Centre for Human Genetics and Department of Clinical Neurology, University of Oxford, Oxford, United Kingdom, ⁶Department of Medical Genetics and Faculty of Medicine, Division of Neurology, University of British Columbia, Vancouver, British Columbia, Canada, ⁷Program in Developmental Therapeutics, Fox Chase Cancer Center, Philadelphia, Pennsylvania, United States of America

Multiple sclerosis (MS) is a chronic progressive, demyelinating condition whose therapeutic needs are unmet, and whose pathoetiology is elusive. We report that transient receptor potential vanilloid-1 (TRPV1) expressed in a major sensory neuron subset, controls severity and progression of experimental autoimmune encephalomyelitis (EAE) in mice and likely in primary progressive MS. TRPV1^{-/-} B6 congenics are protected from EAE. Increased survival reflects reduced central nervous systems (CNS) infiltration, despite indistinguishable T cell autoreactivity and pathogenicity in the periphery of TRPV1-sufficient and -deficient mice. The TRPV1⁺ neurovascular complex defining the blood-CNS barriers promoted invasion of pathogenic lymphocytes without the contribution of TRPV1-dependent neuropeptides such as substance P. In MS patients, we found a selective risk-association of the missense rs877610 TRPV1 single nucleotide polymorphism (SNP) in primary progressive disease. Our findings indicate that TRPV1 is a critical disease modifier in EAE, and we identify a predictor of severe disease course and a novel target for MS therapy.

Online address: <http://www.molmed.org>
doi: 10.2119/molmed.2012.00329

INTRODUCTION

Multiple sclerosis (MS) is a debilitating inflammatory disease of the central nervous system (CNS) characterized by progressive demyelination and axonal damage (1). Its etiology remains unclear, though tissue damage is autoimmune in nature, with several genetic disease risk loci mapped to T cell function (2–4). A key step in disease is thought to be impairment of the blood-

brain barrier (BBB), a logical, but elusive target for therapeutic intervention (5). This physical barrier is established early during embryogenesis and involves a neurovascular unit of pericytes, astrocytes, neurons, endothelial cells, and microglia (PANEM) (6). Normally, tight junctions and low vascular adhesiveness greatly inhibit extravasation into CNS tissue (5). Disruption of the BBB triggers a complex cascade of

events in which the interactive PANEM tissue elements respond to secreted mediators of immune or neuronal derivation (7–9).

A blood-tissue barrier exists in peripheral tissues, although it is not as restrictive as the BBB. Extravasation into peripheral tissues can be induced by activating transient receptor potential vanilloid-1 (TRPV1), a prominent member of the TRP ion channel superfamily (10). TRPV1 is expressed on the major subset of sensory afferent neurons that integrate noxious stimuli including heat and acidity (11–13). The outcome of peripheral TRPV1 activation and consequent cation influx in TRPV1⁺ sensory neuron is two-fold; (i) electric afferent signal transduction to the CNS, generating pain perception and (ii), local efferent release of neuropeptides such as substance P (sP) and calcitonin gene-related peptide (CGRP). Long perceived

*GP and XJL contributed equally to this work.

Address correspondence to H-Michael Dosch, The Hospital for Sick Children, 555 University Avenue, Burton Wing Room 10126, Toronto, ON, Canada. Phone: 416-813-6256; Fax: 416-813-6255; E-mail: michael.dosch@me.com.

Submitted November 9, 2012; Accepted for publication May 8, 2013; Epub (www.molmed.org) ahead of print May 10, 2013.

as largely a heat sensor, TRPV1 is emerging as a major controller of pleiotropic functions in different tissue milieus. Abnormal TRPV1 activity can alter the severity and progression of peripheral inflammatory conditions dramatically, including type 1 diabetes (T1D), colitis and arthritis, through mechanisms largely mediated by its local efferent secretory function: too little in T1D, too much in colitis and arthritis (14–16).

TRPV1 also is expressed within CNS regions, including the spinal cord dorsal horn and areas of the brain (17–21). TRPV1 function in these locations remains a topic of debate. Broad expression patterns have fostered the view that central TRPV1 plays a role in pain processing and thermoregulation, and independent studies have suggested that PANEM cells may all express TRPV1, characterizing the BBB as a TRPV1-rich microenvironment (18,20,22). Activation of TRPV1 by application of the agonist capsaicin directly to the brain disrupts BBB integrity (23), and peripheral TRPV1 stimulation also opens the BBB and blood spinal cord barriers (BSCB) (24), supporting recent evidence that TRPV1 may modify cytokine signaling during CNS neuroinflammation and implying a disease-modifying role (25).

We investigated this possibility with a focus on EAE-autoimmunity. TRPV1^{-/-} mice are dramatically protected from disease, developing minimal and delayed disease onset, reduced clinical scores and reduced demyelination. TRPV1 signaling effectively increases BSCB and BBB permeability, actively promoting inflammatory cell extravasation, which is minimal in the absence of TRPV1. A model is provided to explain how TRPV1 signaling in the PANEM complex may be sustained at body temperature. We conducted parallel studies of patients from the Canadian Collaborative Project on Genetic Susceptibility to Multiple Sclerosis (CCPGSMS), a large and lengthy population-based study (26–28), focusing on the extremely polymorphic TRPV1 locus (29). We found a

significant missense single nucleotide polymorphism (SNP) selection bias in patients with a very progressive disease course, indicating that the unexpected core role of TRPV1 may extend to patients with MS.

MATERIALS AND METHODS

Mice

All mice were purchased from Jackson Laboratories (Bar Harbor, ME, USA) and maintained in our vivarium in a pathogen-free, temperature-controlled environment on a 12 h light:dark cycle. Experiments were performed using age- and gender-matched mice under approved protocols and in agreement with animal ethics guidelines.

Induction and Transfer of EAE

EAE was induced in mice 6–8 weeks old. For active immunization, mice were immunized in each flank with 50 µg of MOG_{35–55} peptide (Alpha Diagnostic, San Antonio, TX, USA) emulsified in CFA (1:1) (Sigma-Aldrich, St. Louis, MO, USA). Where indicated, 200 ng pertussis toxin (Sigma-Aldrich) was given intraperitoneally (IP) on the day of EAE induction and 48 h later. Passive immunization was performed as described (30). Briefly, donor mice were immunized as described above. Draining lymph node cells were removed 8 d after immunization and cultured in the presence of 5 µg/mL MOG_{35–55} peptide for 72 h; 1×10^7 cells were then injected intravenously (IV) into recipient mice along with 200 ng of pertussis toxin (Sigma-Aldrich) IP on the day of injection and 48 h later. For TRPV1 antagonist administration, mice were given 30 mg/kg capsaizepine dissolved in 10% Tween-80 (Sigma-Aldrich), 10% ethanol, and 80% saline on 7 consecutive days. Animals were followed for a minimum of 24 d and disease was scored using the following scale: 0, asymptomatic; 1, limp tail; 2, abnormal righting reflex and/or hind limb weakness; 3, unilateral hind limb paralysis; 4, bilateral hind limb paralysis; 5, moribund or death.

Histology and Immunofluorescence

Spinal cord and brain tissue was dissected at peak disease, 16–18 d after active immunization and 24 d after passive immunization. Tissue was fixed for up to 72 h in 10% buffered formalin before staining with hematoxylin and eosin (H&E) or Luxol fast blue (LFB). Infiltration was scored by a blinded certified pathologist using the following scoring system: 1, normal, with intravascular nonadherent leukocytes; 2, intravascular adherent leukocytes; 3, perivascular infiltration. Demyelination was quantified using ImageJ software analysis (NIH, Bethesda, MD, USA).

Immunoblotting

Mouse spinal cord and brain tissue was dissected and snap frozen. Astrocytes were isolated from neonatal mouse brains as described previously (31) and from C8-D1A cell line (ATCC, Manassas, VA, USA) *in vitro* cultures. Extracted total protein was electrofractionated on 10% acrylamide gels (Invitrogen [Life Technologies, Carlsbad, CA, USA]), blotted, and probed overnight at 4°C with rabbit anti-TRPV1 antibody (1:200, Calbiochem [EMD Millipore, Billerica, MA, USA]) and rabbit anti-β-actin antibody (1:1000, Cell Signaling, Danvers, MA, USA). The following day, bands were visualized using the Western Lightning-ECL kit (PerkinElmer, Waltham, MA, USA).

Proliferation and Cytokine Secretion

Splenocytes or inguinal lymph node cells (4×10^5) were incubated in 96-well plates with HL-1 media (Lonza, Basel, Switzerland) and stimulated with MOG_{35–55} for 72 h. For proliferation experiments, 1 mCi of [³H]thymidine was added for 18 h, prior to harvest and liquid scintillation counting. T cell and B cell specific proliferation was measured as described above following stimulation with 1 µg/mL α-CD3 plus 0.25 µg/mL α-CD28, or 1 µg/mL α-CD40 (BD Pharmingen [BD Biosciences, San Jose, CA, USA]). For cytokine analysis, supernatants were collected after 72 h of culture. IFN-γ, IL-10, and IL-4 (BD Bio-

sciences), IL-12 and TNF- α (eBioscience, San Diego, CA, USA), and IL-17 (R&D Systems, Minneapolis, MN, USA) were measured by enzyme-linked immunosorbent assay (ELISA) according to the manufacturer's protocols.

Flow Cytometry

CNS cells were isolated as described previously (32). Splenocytes or CNS cells (1.5×10^6) were incubated at 4°C for 15 min in 100 μ L 2% fetal bovine serum (FBS)/phosphate-buffered saline (PBS) with 10 μ g/mL Fc-blocker (eBioscience). Cells were incubated for 30 min with the following fluorescent antibodies: CD11b (1:100), CD3 (1:100), CD4 (1:75), CD8 (1:100), B220 (1:100), IgM α L (1:100) (eBioscience), CD11c (1:100), CD62L (1:150), CD44 (1:100) (BD Biosciences), or CD45.2 (1:75) (Invitrogen [Life Technologies]). Samples were run on an LSR-II flow cytometer (BD Biosciences) and FACS plots were analyzed using FlowJo software (Tree Star Inc., Ashland, OR, USA).

Gene Chip

For cDNA gene arrays, RNA from brain and spinal cord was isolated from mice 8 d after immunization using TRIzol Reagent (Invitrogen [Life Technologies]), followed by PureLink RNA Mini Kit (Invitrogen [Life Technologies]). Gene arrays used the Mouse Gene 1.0 ST array (Affymetrix, Santa Clara, CA, USA) and analysis by Expression Console (Affymetrix). Predicted and unknown genes were excluded from analysis.

Blood Spinal Cord/Brain Barrier Analysis

Evans Blue dye flux into brain and spinal cord tissue was determined as described (24). Briefly, 4 mL/kg of 2% Evans Blue dye (Sigma-Aldrich) was injected IV and after 2 h animals were perfused with PBS. The spinal cord and supraspinal tissues were immediately dissected, removing the dura mater. The lumbar spinal cord, thoracic spinal cord, brain stem, cerebellum and frontal cortex were further dissected and weighed. Tissue was incubated in formamide (Sigma-Aldrich)

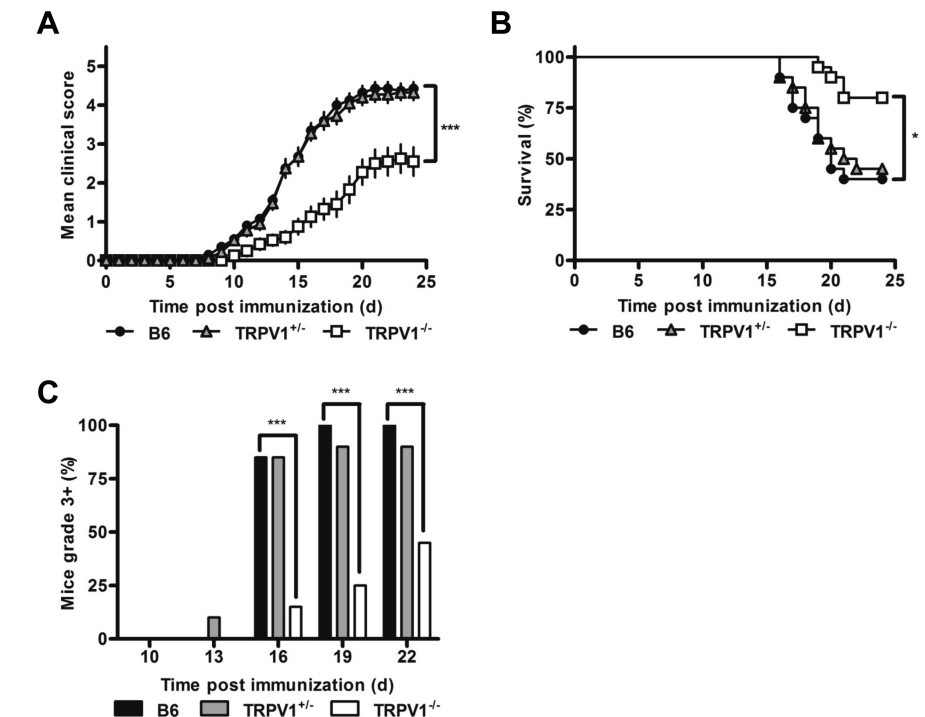


Figure 1. TRPV1^{-/-} mice are protected from severe EAE. (A) Daily clinical scores of B6, TRPV1^{+/-} and TRPV1^{-/-} mice following immunization with MOG₃₅₋₅₅ peptide and pertussis toxin (n = 20 per group, ***p < 0.0001). (B) Survival curve following induction of EAE with pertussis toxin (n = 20 per group, *p < 0.05). (C) Proportion of mice with severe EAE (n = 20 per group, ***p < 0.0001).

at 60° C for 72 h, and dye concentration in extracts was determined by spectrophotometry (620 nm) in a 96-well plate reader.

To measure permeability of large molecule (infrared-labeled IgG), 5 μ g/g of donkey anti-goat IgG, IRDye 800CW labeled (LI-COR Biosciences, Lincoln, NE, USA) was injected IV and, after 30 min, animals were perfused with PBS. Spinal cord and supraspinal tissues were immediately dissected and scanned with an Odyssey Infrared Imager (LI-COR Biosciences).

For magnetic resonance imaging, a multichannel 7.0 T magnet was used to acquire *in vivo* 2D T1-weighted MR images (100 μ m in-plane resolution) of the thoracic and lumbar spinal cord. Mice were injected with a bolus of Gd-DTPA (1.5 mmol/kg) IP and imaged at 1% isoflurane according to established protocols. Quantitative measurements of sig-

nal intensity were determined by normalizing the spinal cord intensity to the average intensity of two phantoms included in each coil (microcapillary tubes containing 1% Gd-DTPA in agar).

Human Subjects

All subjects used in the study were ascertained through the ongoing Canadian Collaborative Project on the Genetic Susceptibility to MS (CCPGSMS), as described (26–28). DNA and anonymized clinical charts from a total of 163 sporadic MS patients were identified for analysis. The disability of the sporadic MS patients was assessed carefully and recorded at study entry with the Expanded Disability Status Scale (EDSS) determined by neurologists involved in the CCPGSMs. Here, patients were classified as having either “benign” or “malignant” MS based on EDSS scores sustained or achieved over designed time

intervals. The benign MS cases ($n = 112$) fell into the relapsing-remitting clinical subtype where minimal disability (that is, EDSS ≤ 3) was sustained over a period >20 years from disease onset. By contrast, the malignant MS cases ($n = 51$), a subgroup of MS patients acquiring significant disability (that is, EDSS >6 ; the need for a walking aid or worse) within 5 years of disease onset, had the primary progressive form of the disease.

Genotyping

Total genomic DNA, extracted from whole blood as part of the CCPGMS (33), was used to type SNPs. Genotyping of SNPs was performed using the Sequenom MassEXTEND protocol (www.sequenom.com). Only conservative and moderate genotyping calls were accepted in this study. Samples having aggressive or low probability quality genotypes were reanalyzed.

Statistical Analysis

Statistical significance between two means was assessed by Mann-Whitney and unpaired t tests, and Welch correction was employed where appropriate. Analysis of curves was performed using two-way analysis of variance (ANOVA). Human data was analyzed using the PLINK analysis package (34). Statistical significance was two-tailed and set at 5%, with error bars showing a single standard deviation.

All supplementary materials are available online at www.molmed.org.

RESULTS

TRPV1 is Pathogenic in EAE

To determine the role of TRPV1 in EAE progression, we induced disease in B6 mice, and TRPV1^{+/-} and TRPV1^{-/-} congenics. Spinal cord TRPV1 expression in heterozygous mice was 35% of wild type B6 levels, providing a valuable intermediate (Supplementary Figure 1A). In the classical MOG-EAE model, where immunized mice also receive IP pertussis toxin, both B6 and TRPV1^{+/-} congenics

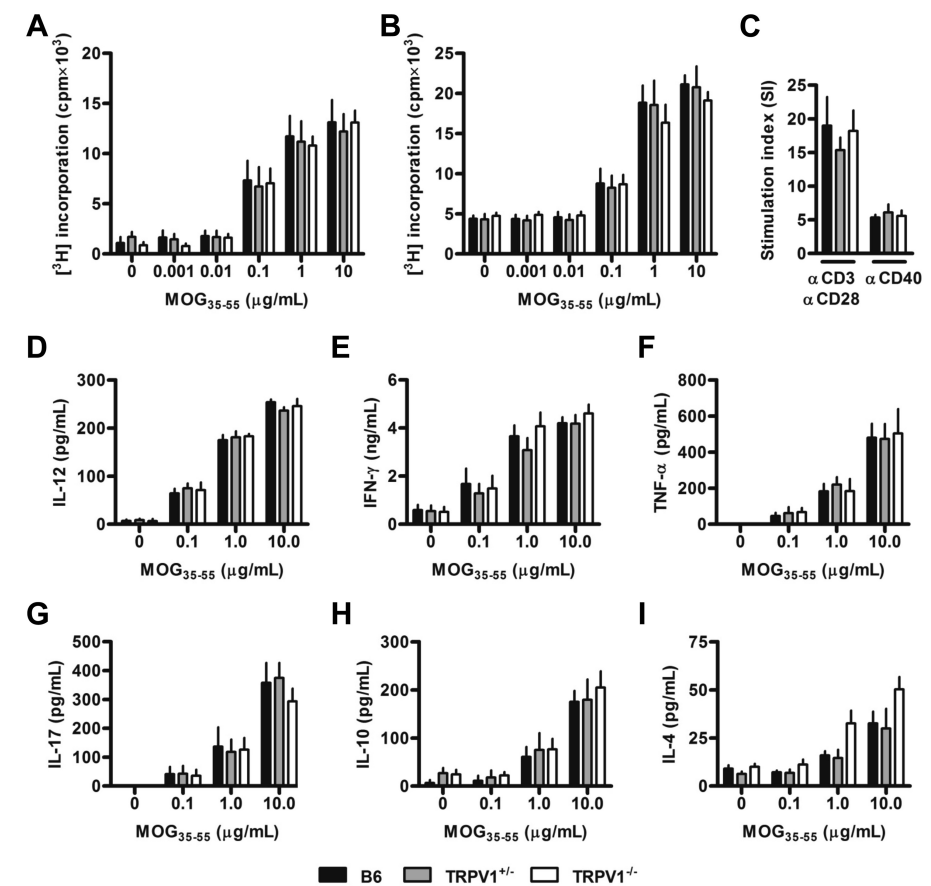


Figure 2. TRPV1 expression does not affect the effectiveness of MOG₃₅₋₅₅ immunization. (A) Proliferation following MOG₃₅₋₅₅ peptide restimulation of inguinal lymph node cells ($n = 4$ per group) from B6, TRPV1^{+/-} and TRPV1^{-/-} mice euthanized 8–10 d after immunization. (B) Proliferation following restimulation of splenocytes 16–18 d after immunization ($n \geq 9$ per group). (C) Mean stimulation index of splenocytes from naive mice stimulated with α -CD3 and α -CD28 or α -CD40 antibodies ($n = 5$ per group). (D–I) Production of IL-12 (D), IFN- γ (E), TNF- α (F), IL-17 (G), IL-10 (H) and IL-4 (I) by splenocytes following MOG₃₅₋₅₅ peptide restimulation ($n \geq 5$ per group).

progressed to severe disease rapidly, while TRPV1^{-/-} mice exhibited strong protection (Figure 1A). High proportions (~60%) of wild type and TRPV1^{+/-} mice were moribund and euthanized before the end of the 24 d observation period, whereas only few TRPV1^{-/-} mice reached that stage, later in the disease course (Figures 1B, C). TRPV1 expression levels thus correlated with disease penetrance, day of disease onset, maximum clinical disease scores, and mortality (see Figures 1A–C, Supplementary Table 1).

We also induced disease via active immunization with MOG₃₅₋₅₅ peptide, with-

out the classical injections of pertussis toxin, generating mild to moderate disease scores in B6 mice over a 40-d period after immunization, while TRPV1^{-/-} mice were essentially asymptomatic. TRPV1^{+/-} heterozygotes developed intermediate disease scores (Supplementary Figure 1B), suggestive of a gene dose effect.

TRPV1^{-/-} Mice Generate Systemic Pathogenic Autoreactivity but Fail to Infiltrate the CNS

B6, TRPV1^{+/-} and TRPV1^{-/-} mice are immunocompetent and show no obvious differences in the composition of second-

ary lymphoid tissues (Supplementary Figures 2A–D). Nevertheless, we investigated if TRPV1 expression influenced the efficacy of MOG₃₅₋₅₅ immunization, conceivably explaining different disease susceptibilities. Draining lymph node (see Figure 2A) and spleen cells (see Figure 2B) of immunized B6, TRPV1^{+/-} and TRPV1^{-/-} mice proliferated to a similar extent when stimulated with a 5-log range of MOG₃₅₋₅₅ peptide doses, suggesting similar effector cell pool sizes and affinity spectra in the three mouse lines. No differences were observed following polyclonal T or B cell activation by α -CD3 plus α -CD28 or α -CD40 antibodies (see Figure 2C). MOG₃₅₋₅₅-induced cytokine secretory profiles also were comparable in the three strains, with no differences found in those relevant to T_H1, T_H17 or T_H2 responses (Figures 2D–I).

In addition, cellularities were similar in spleen and draining inguinal lymph nodes before and after immunization (Figure 3A), collectively confirming that the induction of anti-MOG₃₅₋₅₅ immune responses were indistinguishable. However, the ability of pathogenic MOG₃₅₋₅₅-activated cells to infiltrate the CNS was dramatically reduced in TRPV1^{-/-} mice (Figure 3B). Differences were observed in absolute numbers of tissue-infiltrating cells including total lymphocytes, CD4⁺ and CD8⁺ T cells, and B cells (see Figure 3B). Interestingly, the relative proportions of CNS-invasive lymphocyte subsets did not differ between B6 and TRPV1^{-/-} mice, including regulatory CD4⁺ Foxp3⁺ cells (Figure 3C), demonstrating a role for TRPV1 in general tissue access rather than involvement in sublineage-selective interactions.

B6 mice euthanized at peak disease displayed marked infiltration in the perivascular regions of both the brain and spinal cord that extended deeply into surrounding tissue, but much reduced infiltration was noted in TRPV1^{-/-} mice (Figures 4A, B), corresponding well to the much reduced numbers extracted (see Figure 3B). Luxol fast blue staining of areas rich in compact myelin, revealed large lacunar areas of myelin loss in dis-

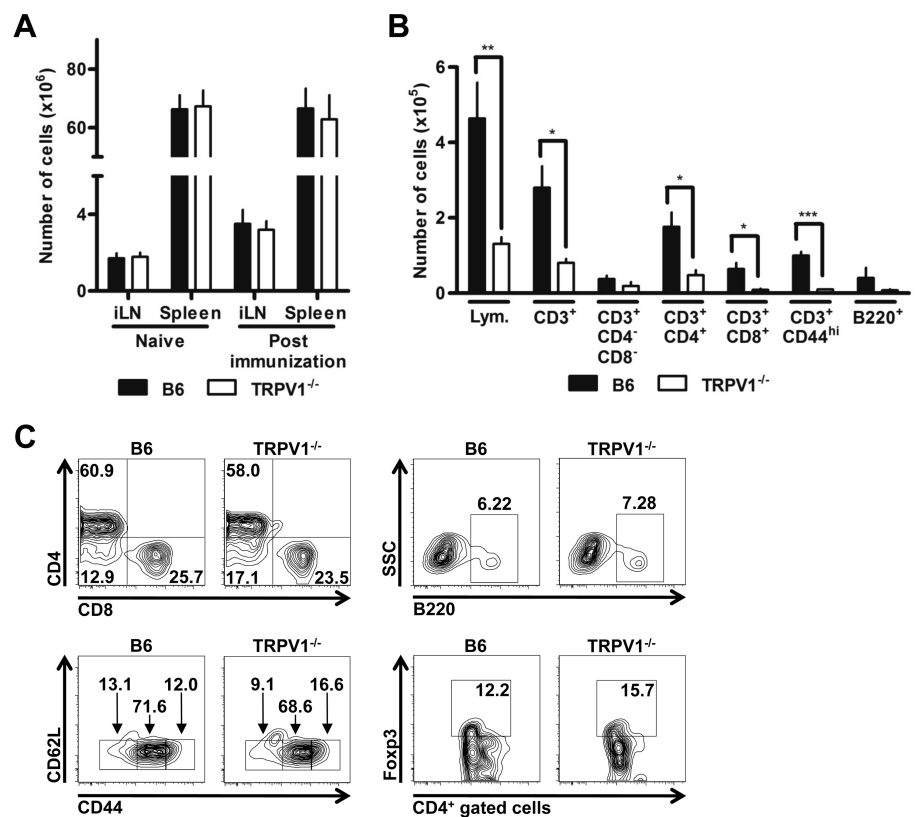


Figure 3. TRPV1^{-/-} mice show reduced CNS infiltration. (A) Cell counts of inguinal lymph node and spleen prior to and following MOG₃₅₋₅₅ peptide immunization of B6 and TRPV1^{-/-} mice ($n = 9$ per group). (B) Quantification of lymphocytes in the CNS by flow cytometry ($n \geq 3$ per group, * $p < 0.05$, ** $p < 0.01$, *** $p < 0.001$). (C) Representative FACS plot showing distribution of cells within the CNS; CD4⁺ and CD8⁺ cells previously gated on CD3⁺ cells (upper left), CD62L⁺ and CD44⁺ cells previously gated on CD3⁺ cells (lower left), B220⁺ cells (upper right), FoxP3⁺ cells previously gated on CD4⁺ cells (lower right).

eased wild type mice (see Figure 4A). In TRPV1^{-/-} mice, such lesions were small and sparse, equivalent to a ~3.5-fold reduction in demyelinated areas (Figure 4C). As suggested by similar clinical disease scores, B6 and TRPV1^{+/-} mice were indistinguishable in their infiltration density, distribution and demyelination (data not shown). Protection in TRPV1^{-/-} mice correlated with the inability of infiltrating cells in these mice to penetrate deep into surrounding tissue. TRPV1^{-/-} mice showed a higher proportion of vessels in which leukocytes were nonadherent or adherent but intravascular and unable to leave the blood compartment (Figure 4D), explaining disease protection and reduced demyelination.

Adoptive Transfer of EAE Fails in TRPV1^{-/-} Mice

In vitro MOG₃₅₋₅₅-restimulated cells ($\times 10^7$) from immunized B6 or TRPV1^{-/-} mice were IV injected into naive B6 mice to produce, within 3 wks, a robust and severe form of EAE, sustained over a 40-d observation period (Figure 5A). By contrast, injection of the same preparation of cells into TRPV1^{-/-} recipients, regardless of the donor, failed to generate similar disease penetrance (see Figure 5A). Most TRPV1^{-/-} recipients showed no clinical symptoms, and disease in mice with minor symptoms resolved quickly without progression. Intravenous adoptive transfer into wild type B6 mice generated lymphocyte infiltration in the brain and

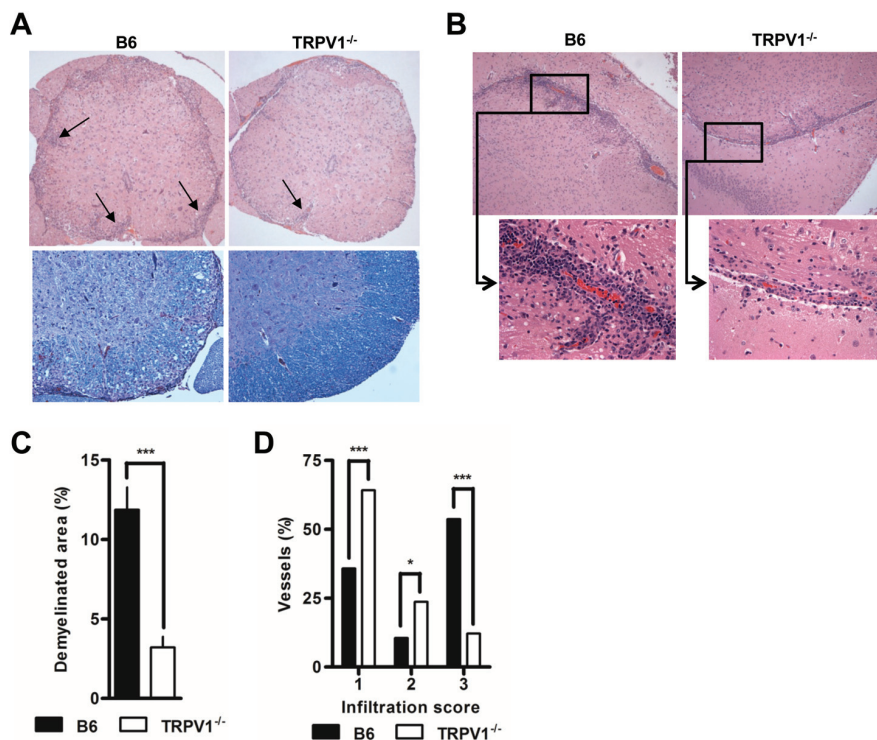


Figure 4. TRPV1 expression correlates to infiltration and demyelination. (A) Representative spinal cord sections stained with H&E (upper) and LFB (lower), original magnification 20 \times . (B) Representative brain sections stained with H&E, original magnification 20 \times , and 40 \times for smaller insets. (C) Quantification of demyelinated areas of spinal cord tissue from B6 and TRPV1^{-/-} mice 16–18 d after immunization ($n = 5$ per group, $p < 0.0001$). (D) Blinded quantification of cellular infiltration in B6, TRPV1^{+/-}, and TRPV1^{-/-} mice euthanized 16–18 d after immunization ($n \geq 95$ per group, * $p < 0.05$, ** $p < 0.01$, *** $p < 0.001$).

spinal cord (Figures 5B, C), as early as d 4 after injection, when greater total numbers of B220⁺ B cells and CD3⁺ T cells were already tissue-invasive, regardless of whether or not recipients were injected with pertussis toxin (Figures 5D, E). Quantification of lymphocytes that were able to access the CNS revealed a >100% difference between B6 and TRPV1^{-/-} recipients (Figure 5F). Given that TRPV1^{-/-} recipients are essentially unable to permit progressive pathogenicity, TRPV1 becomes the fundamental gatekeeper for *in vivo* disease development.

BSCB and BBB Collapse in EAE Is TRPV1-Dependent and Requires Lymphocytes

Given the intimate proximity of TRPV1⁺ cellular PANEM elements at the BBB and BSCB, we monitored barrier in-

tegrity during EAE progression. We detected no increase in the permeability of Evans Blue prior to d 3 after immunization (Figures 6A, B). Evans Blue extravasation following injection of MOG_{35–55} or of pertussis toxin alone was similar in brain and spinal cord regions of B6 and TRPV1^{-/-} mice, rarely, if at all, exceeding baseline d 0 levels (Figures 6A, B). However, after immunization with MOG plus pertussis toxin, permeability was massive by d 11, particularly in the spine of B6 mice (Figures 6A–C) and perhaps reminiscent of the recently discovered lumbar BSCB tissue entry pathway (35). Significantly lower leakage levels were seen in TRPV1^{-/-} mice, closely resembling lymphocyte-free RAG1^{-/-} B6 congenics (Supplementary Figure 3). These observations extended to large molecule leakage, demonstrated by infrared-la-

beled IgG, with results comparable to Evans Blue extravasation (Figures 6D, E).

While large molecule permeability is dependent on transcytosis, we questioned the permeability of small molecules that normally depend on processes such as diffusion. The blood-spinal cord barrier is normally impermeable to magnetic resonance (MR) contrast agents such as the small (260Da) Gadolinium-DTPA reagent, but in cases of barrier disruption will appear hyperintense in T1-weighted MR images (36). MRI detected CNS edema sensitively but almost equally during EAE in B6 and in protected TRPV1^{-/-} mice, identifying a shared inflammatory element that is, however, self-limiting and without progressive tissue damage in the absence of TRPV1 (Figure 6F).

We demonstrate TRPV1 expression within astrocytes isolated from the brains of B6 mice and within the astrocyte cell line C8-D1A (Supplementary Figure 4A), similar to previous reports (18,20). This PANEM cell type plays a fundamental role in BSCB and BBB permeability, and further investigation into astrocyte functions mediated by TRPV1 is warranted. We also noted that TRPV1 expression levels within the CNS remain unchanged during the course of EAE (Supplementary Figure 4B), despite previous reports of altered expression in other disease states (37). Conversely, the expression of numerous hematopoietic cell lineage genes is upregulated significantly compared with TRPV1^{-/-} mice, serving as an independent corollary of our data where B6 mice developed severe disease (Supplementary Figures 5A–C). B6 mice also showed increased transcription of numerous genes typically restricted to neuronal or nonhematopoietic tissue (Supplementary Figure 5D), providing a number of opportunities for future research investigating BSCB and BBB integrity. Collectively, TRPV1-dependent BSCB and BBB compromise per se requires antigen, adjuvant and lymphocytes, hallmarks of a cognate immune response.

Given the role of TRPV1 in promoting the severity of encephalitis, we questioned if a TRPV1 antagonist could elicit

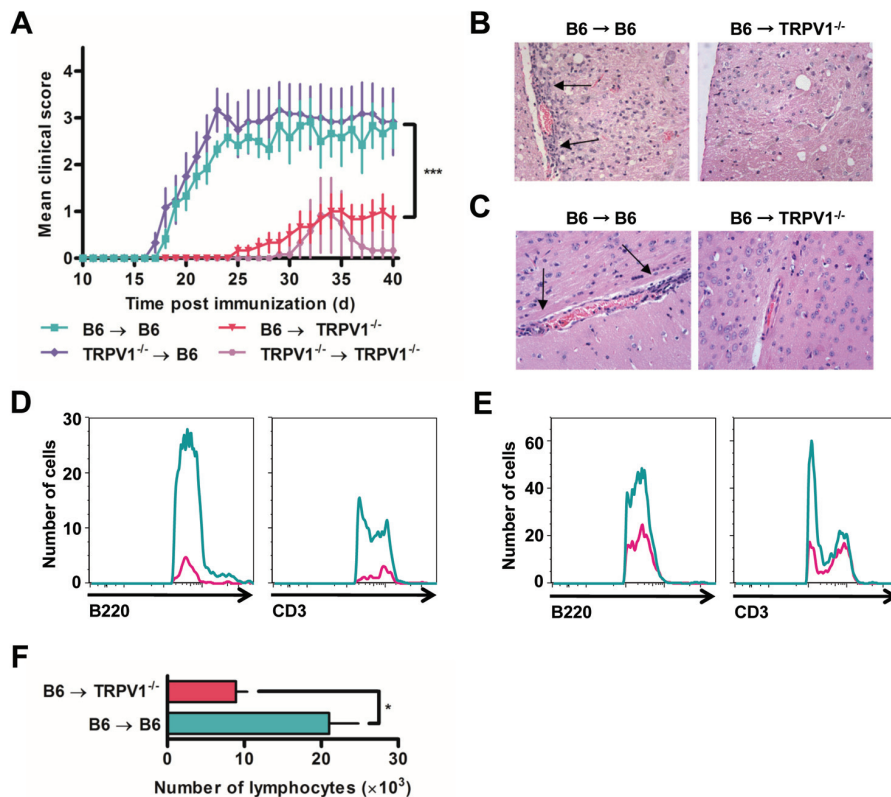


Figure 5. TRPV1^{-/-} mice are protected from adoptive transfer of EAE. (A) Daily clinical scores of B6 and TRPV1^{-/-} recipient mice following the adoptive transfer of 1×10^7 donor cells ($n = 6$ per group, $***p < 0.0001$). (B–C) Representative H&E stained spinal cord (B) and brain (C) sections from B6 and TRPV1^{-/-} recipient mice 24 d after transfer, original magnification 40 \times . (D–E) Number of B220⁺ and CD3⁺ cells within the CNS 4 d after transfer of B6 cells without (D) and with (E) injections of pertussis toxin. (F) Quantification of lymphocytes recovered from the CNS following adoptive transfer of B6 cells ($n = 3$ per group, $*p < 0.05$).

disease protection. We administered capsaizepine subcutaneously and intranasally from d 0 to d 6 after immunization at a dose effective in other models (38). Despite our attempts, we found no significant difference between B6 mice treated with the antagonist and those, which received vehicle alone (Supplementary Figure 6), though we believe that adjustments to the dose, timing, and possibly the antagonist itself, may be prudent future approaches.

A Role for TRPV1, but Not Tac1, in EAE and MS

To further elucidate the mechanism explaining protection seen in TRPV1^{-/-} mice, we induced active EAE in Tac1^{-/-} mice, which are deficient in one of the

main effector neuropeptides secreted following TRPV1 activation, sP. Tac1^{-/-} mice did not have a comparable impact on disease, with clinical scores aligning very closely with B6 mice (Figure 7).

As we were striving to identify links between mouse models and human disease, it was important that the studies described above be probed for possible parallels in MS patients. We chose a genomic approach, based on the extreme allelic polymorphism of the human TRPV1 locus (29), and analyzed a cohort of MS patients from the CCPGMS trial (28). Measuring allelic variation in TRPV1 and Tac1 genes, single nucleotide polymorphisms (SNPs) were compared in genomic DNA from MS cases at opposite extremes of long-term clinical out-

comes, as assessed by the EDSS. The MS cases selected represent the prognostic best 5%, classified as “benign” MS, and the worst 5%, classified as “malignant” MS. The difference between groups is dramatically reflected by mean age of onset and mean duration of disease (Table 1). Specific SNPs in the TRPV1 locus were either significantly overrepresented in DNA of patients with malignant MS or underrepresented in the genomes of patients with benign MS (Table 1). Each possible scenario is being tested in larger DNA collections, but the data described here provide strong first evidence for a disease course–associated role of TRPV1 in MS. No significant disease association was found following the analysis of two SNPs present in the Tac1 gene (Table 1), in agreement with mouse studies.

DISCUSSION

Our inability to accurately predict the clinical course of MS, and subsequently tailor patient therapy, reflects our failure to fully understand disease etiology and pathogenesis. Here we identify TRPV1 as a major progression element in murine EAE and as a likely participant in MS.

We went to considerable efforts to determine if, as in T1D, the pathogenic role of TRPV1 had no detectable impact on disease-promoting autoimmune profiles, including numeric, functional and subset distributions of autoreactive lymphocyte lineages. TRPV1 may be expressed on antigen presenting cells (39,40), but we conclude that it has negligible effects during the initiation and progression phases of EAE autoimmunity. Conversely, the numeric size of T cell and B cell infiltrates in the CNS remains minuscule in the absence of TRPV1, despite equal pool sizes of disease-associated lymphocytes systemically. Similar results were observed following adoptive transfer of highly activated autoreactive cells, where B6 recipients developed acute disease and TRPV1^{-/-} recipients were almost entirely protected with sparse cellular infiltration while their lymphocytes were highly pathogenic in B6 hosts.

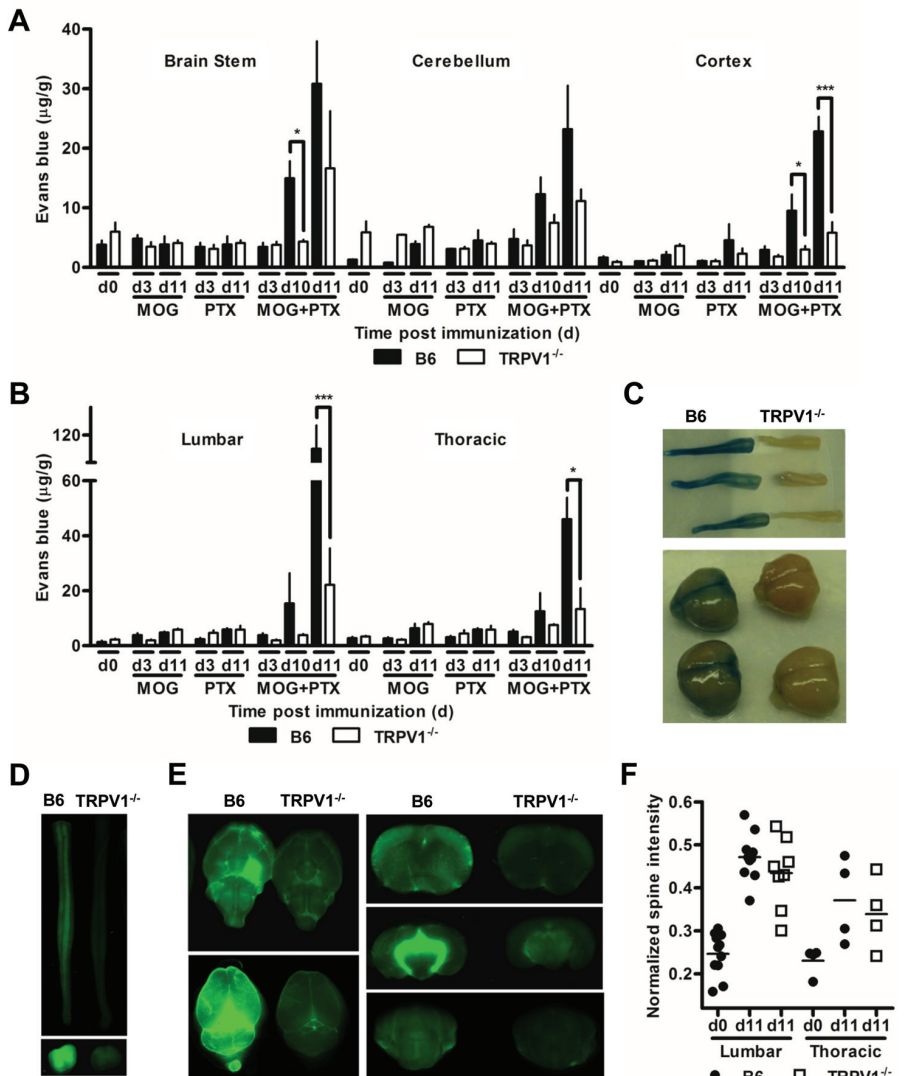


Figure 6. TRPV1 increases the permeability of the BBB and BSCB. (A–B) Quantification of Evans Blue in regions of the brain (A, $n = 5$ per group, $*p < 0.05$, $***p < 0.001$) and the spinal cord (B, $n = 5$ per group, $*p < 0.05$, $***p < 0.001$) of B6 and TRPV1^{-/-} mice at indicated time points after induction of EAE, or after injection with MOG₃₅₋₅₅ or pertussis toxin alone. (C) Representative images of brain and spinal cord tissue dissected from B6 and TRPV1^{-/-} mice 11 d after immunization following Evans Blue injection. (D) Representative images of B6 and TRPV1^{-/-} whole spinal cord (upper) and sectioned spinal cord (lower) following injection of infrared-labeled IgG 11 d after immunization. (E) Representative images of B6 and TRPV1^{-/-} whole brain (upper left: coronal and lower left: transverse) and sectioned brain (upper, middle, and lower right) following injection of infrared-labeled IgG 11 d after immunization. (F) Average intensity readings in the lumbar and thoracic regions of the spine following MRI of B6 and TRPV1^{-/-} mice 11 d after immunization.

Our attention therefore shifted to the barriers that control lymphocyte egress into the CNS. Dramatic breakdown of BSCB and BBB integrity preceding peak disease was absent in TRPV1^{-/-} mice,

suggesting that TRPV1 itself is a participant in the PANEM cluster that grants passage to effector cells. This effect on permeability was not all encompassing, as small molecule permeability was still

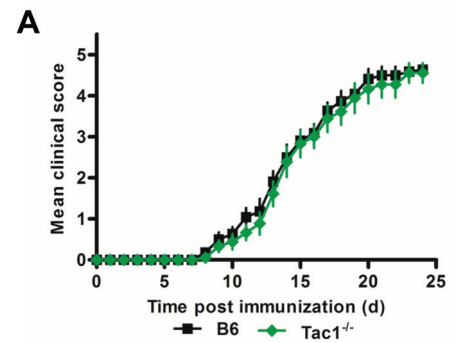


Figure 7. Tac1^{-/-} mice are not protected from EAE. Daily clinical scores of B6 and Tac1^{-/-} mice following immunization with MOG₃₅₋₅₅ peptide and pertussis toxin ($n \geq 9$ per group).

intact irrespective of TRPV1 expression. We provide data suggesting that one of the cell types mediating this effect may be astrocytes, and the functional consequences of this expression during EAE should be examined further. Interestingly, a relationship between TRPV1 and CNS access also is seen in nonobese diabetic (NOD) mice (41), a mouse strain found to carry a hypofunctional TRPV1 mutant gene (14).

Genetic deletion of TRPV1 produced significant disease protection in B6 MOG-EAE, including day of onset, maximum clinical scores and overall survival. Fittingly, one major genomic interval (*ae7*) that modulates the severity and duration of clinical signs during EAE (42,43) includes TRPV1. It is likely that the contribution of TRPV1 in this locus is considerable, as precedence has been shown in another T cell-mediated autoimmune disease, T1D (*idd4.1*) (14). Intermediate disease scores in TRPV1^{+/-} mice support the idea that therapeutic targeting of TRPV1 by antagonists would, on face value, have a rationale, but might have to suppress significantly more than 65% of TRPV1 activity, that is, the levels observed here in TRPV1^{+/-} heterozygotes. This may explain why our attempts to limit disease severity using capsaizepine were unsuccessful. The efficacy of additional TRPV1 antagonists, currently approved for clinical use (44),

Table 1. Tac1 and TRPV1 SNP frequencies in benign and malignant MS patients.

Clinical/demographic details	Benign MS	Malignant MS				
Sample size (n)	112	51				
Sex ratio (F:M)	87:25 (3.48:1)	30:21 (1.43:1)				
Mean age of onset (y)	25.1	37.3				
Mean duration of disease (y)	26	3.6				
SNP	Frequency (benign MS)	Frequency (malignant MS)	Allele tested	Chi	p Value (nominal)	Odds ratio (95% CI)
rs6465606 (Tac1)	0.25	0.29	A	0.81	0.37	1.21 (0.80–1.84)
rs4526299 (Tac1)	0.16	0.15	T	0.15	0.70	0.90 (0.54–1.52)
rs877610 (TRPV1)	0.04	0.09	T	5.43	0.02	2.43 (1.13–5.21)
rs8065080 (TRPV1)	0.34	0.30	C	0.53	0.47	0.86 (0.58–1.29)
rs224534 (TRPV1)	0.35	0.44	A	3.18	0.07	1.42 (0.97–2.07)

should be investigated further to treat EAE and MS.

On the basis of observations in the EAE model, we analyzed a total of 163 individuals from the CCPGMS program who were stratified into two groups on opposite ends of the clinical spectrum, thus examining TRPV1 and Tac1 (sP-coding) genes as disease modifiers rather than determinants of overall disease risk, a comparison that generally yields more modest associations (45). Patients with the most severe progression showed an overrepresentation of certain TRPV1 SNPs. The nonsynonymous mutation rs877610 is located within the intracellular C-terminal domain of TRPV1 in proximity to known binding sites, while rs224534, which also results in an amino acid change, lies within an extracellular region between the first two transmembrane domains. It will take considerable sequencing efforts to more fully characterize the allelic heterogeneity of TRPV1 in general and in patient populations such as MS. Furthermore, it will be important to determine if these alleles render TRPV1 activity hypofunctional or hyperfunctional. Even though sP is functionally linked to TRPV1, Tac1 SNPs showed no bias in our patient population. In retrospect, our failure to find relevant Tac1 SNPs should not surprise, given our comparison within a disease population rather than comparing patients with normal controls as before (46,47), and it coincides with the lack of EAE protection observed here in Tac1^{-/-} mice.

We have made several comparisons between encephalitis and T1D, given the relatively high prevalence, in some populations, of MS and T1D comorbidity (48). The brain has the highest energy budget among organs: 20% of the total energy for 2% of body mass (49). To use abundant glucose, the PANEM complex must sustain high volume one-way traffic of insulin that makes the PANEM complex an insulin-rich milieu comparable to some extent to pancreatic islets. Insulin receptor ligation by TRPV1⁺ terminals raises TRPV1 currents, resetting activation thresholds to room temperature (50,51). Thus, there is potential for TRPV1 activation outside of its normal temperature constraints where specific TRPV1 alleles may confer a risk scenario. Alternatively, lipid TRPV1 agonists also may contribute to this process, as they have been reported to be upregulated in the brain and spinal cord during neuroinflammatory conditions such as EAE (52,53). The presence of enzymes responsible for catalyzing the biosynthesis of these endogenous agonists in the brain has also been reported previously (54). Anandamide and palmitoylethanolamide can either activate or desensitize TRPV1 (55), and their actions on TRPV1 within the CNS in the context of encephalitis should be strongly considered (56).

CONCLUSION

Collectively, our data make TRPV1 a prominent factor controlling disease progression/severity in EAE. Although

numerically limited, our human observations employed a stringently selected subset of a large and well-characterized, population-based patient cohort, linking differences in disease course to polymorphisms in the human TRPV1 locus. While considerable work will be required to characterize the TRPV1 locus in MS patients and their relatives, allele sequences are likely to be identified that can predict severe course and thus rationalize aggressive therapies. TRPV1 continues to be a challenging drug target in humans (57,58), yet TRPV1-targeted treatments might have the potential to replace drug targeting of the immune system with its associated toxicities.

ACKNOWLEDGMENTS

This work was supported by grants from the Canadian Institutes of Health Research (CIHR), the MS Society of the United Kingdom, and the MS Society of Canada Scientific Research Foundation. We thank L Morikawa for excellent assistance with histopathology. G Paltser is a recipient of awards from CIHR and the Banting and Best Diabetes Centre (Toronto). LS Cahill is a recipient of a CIHR postdoctoral fellowship.

DISCLOSURE

The authors declare that they have no competing interests as defined by *Molecular Medicine*, or other interests that might be perceived to influence the results and discussion reported in this paper.

REFERENCES

- Noseworthy JH, Lucchinetti C, Rodriguez M, Weinshenker BG. (2000) Multiple sclerosis. *N. Engl. J. Med.* 343:938–52.
- Hafler DA, et al. (2007) Risk alleles for multiple sclerosis identified by a genomewide study. *N. Engl. J. Med.* 357:851–62.
- Weber F, et al. (2008) IL2RA and IL7RA genes confer susceptibility for multiple sclerosis in two independent European populations. *Genes Immun.* 9:259–63.
- Caillier SJ, et al. (2008) Uncoupling the roles of HLA-DRB1 and HLA-DRB5 genes in multiple sclerosis. *J. Immunol.* 181:5473–80.
- Bennett J, et al. (2010) Blood-brain barrier disruption and enhanced vascular permeability in the multiple sclerosis model EAE. *J. Neuroimmunol.* 229:180–91.
- Neuwelt EA. (2004) Mechanisms of disease: the blood-brain barrier. *Neurosurgery.* 54:131–40; discussion 141–2.
- Kebir H, et al. (2007) Human TH17 lymphocytes promote blood-brain barrier disruption and central nervous system inflammation. *Nat. Med.* 13:1173–5.
- Yu F, Kamada H, Niizuma K, Endo H, Chan PH. (2008) Induction of mmp-9 expression and endothelial injury by oxidative stress after spinal cord injury. *J. Neurotrauma.* 25:184–95.
- Annunziata P, Cioni C, Santonini R, Paccagnini E. (2002) Substance P antagonist blocks leakage and reduces activation of cytokine-stimulated rat brain endothelium. *J. Neuroimmunol.* 131:41–9.
- Koltzenburg M. (2004) The role of TRP channels in sensory neurons. *Novartis Found. Symp.* 260:206–13; discussion 213–20, 277–9.
- Caterina MJ, et al. (1997) The capsaicin receptor: a heat-activated ion channel in the pain pathway. *Nature.* 389:816–24.
- Patwardhan AM, et al. (2010) Heat generates oxidized linoleic acid metabolites that activate TRPV1 and produce pain in rodents. *J. Clin. Invest.* 120:1617–26.
- Bohlen CJ, et al. (2010) A bivalent tarantula toxin activates the capsaicin receptor, TRPV1, by targeting the outer pore domain. *Cell.* 141:834–45.
- Razavi R, et al. (2006) TRPV1+ sensory neurons control beta cell stress and islet inflammation in autoimmune diabetes. *Cell.* 127:1123–35.
- Kimball ES, Wallace NH, Schneider CR, D'Andrea MR, Hornby PJ. (2004) Vanilloid receptor 1 antagonists attenuate disease severity in dextran sulphate sodium-induced colitis in mice. *Neurogastroenterol. Motil.* 16:811–8.
- Szabo A, et al. (2005) Role of transient receptor potential vanilloid 1 receptors in adjuvant-induced chronic arthritis: in vivo study using gene-deficient mice. *J. Pharmacol. Exp. Ther.* 314:111–9.
- Mezey E, et al. (2000) Distribution of mRNA for vanilloid receptor subtype 1 (VR1), and VR1-like immunoreactivity, in the central nervous system of the rat and human. *Proc. Natl. Acad. Sci. U. S. A.* 97:3655–60.
- Doly S, Fischer J, Salio C, Conrath M. (2004) The vanilloid receptor-1 is expressed in rat spinal dorsal horn astrocytes. *Neurosci. Lett.* 357:123–6.
- Roberts JC, Davis JB, Benham CD. (2004) [3H]Resiniferatoxin autoradiography in the CNS of wild-type and TRPV1 null mice defines TRPV1 (VR-1) protein distribution. *Brain Res.* 995:176–83.
- Toth A, et al. (2005) Expression and distribution of vanilloid receptor 1 (TRPV1) in the adult rat brain. *Brain Res. Mol. Brain Res.* 135:162–8.
- Cristino L, et al. (2006) Immunohistochemical localization of cannabinoid type 1 and vanilloid transient receptor potential vanilloid type 1 receptors in the mouse brain. *Neuroscience.* 139:1405–15.
- Schilling T, Eder C. (2009) Importance of the non-selective cation channel TRPV1 for microglial reactive oxygen species generation. *J. Neuroimmunol.* 216:118–21.
- Hu DE, Easton AS, Fraser PA. (2005) TRPV1 activation results in disruption of the blood-brain barrier in the rat. *Br. J. Pharmacol.* 146:576–84.
- Beggs S, Liu XJ, Kwan C, Salter MW. (2010) Peripheral nerve injury and TRPV1-expressing primary afferent C-fibers cause opening of the blood-brain barrier. *Mol. Pain.* 6:74.
- Musumeci G, et al. (2011) Transient receptor potential vanilloid 1 channels modulate the synaptic effects of TNF-alpha and of IL-1beta in experimental autoimmune encephalomyelitis. *Neurobiol. Dis.* 43:669–77.
- DeLuca GC, et al. (2007) An extremes of outcome strategy provides evidence that multiple sclerosis severity is determined by alleles at the HLA-DRB1 locus. *Proc. Natl. Acad. Sci. U. S. A.* 104:20896–901.
- Ramagopalan SV, et al. (2007) Autoimmune disease in families with multiple sclerosis: a population-based study. *Lancet Neurol.* 6:604–10.
- Sadovnick AD, Risch NJ, Ebers GC. (1998) Canadian collaborative project on genetic susceptibility to MS, phase 2: rationale and method. Canadian Collaborative Study Group. *Can. J. Neurol. Sci.* 25:216–21.
- Dorfman R, Tsui H, Salter MW, Dosch HM. (2010) TRPV1 Genetics. In: *Vanilloid Receptor TRPV1 in Drug Discovery*. Arthur G, Faltinek CR (eds.) J Wiley & Sons, Hoboken, NJ, pp. 134–149.
- Kuwabara T, et al. (2009) CCR7 ligands are required for development of experimental autoimmune encephalomyelitis through generating IL-23-dependent Th17 cells. *J. Immunol.* 183:2513–21.
- Luo Y, Fischer FR, Hancock WW, Dorf ME. (2000) Macrophage inflammatory protein-2 and KC induce chemokine production by mouse astrocytes. *J. Immunol.* 165:4015–23.
- Winer S, et al. (2009) Normalization of obesity-associated insulin resistance through immunotherapy. *Nat. Med.* 15:921–9.
- Aulchenko YS, et al. (2008) Genetic variation in the KIF1B locus influences susceptibility to multiple sclerosis. *Nat. Genet.* 40:1402–3.
- Purcell S, et al. (2007) PLINK: a tool set for whole-genome association and population-based linkage analyses. *Am. J. Hum. Genet.* 81:559–75.
- Arima Y, et al. (2012) Regional neural activation defines a gateway for autoreactive T cells to cross the blood-brain barrier. *Cell* 148:447–57.
- Schellenberg AE, Buist R, Yong VW, Del Bigio MR, Peeling J. (2007) Magnetic resonance imaging of blood-spinal cord barrier disruption in mice with experimental autoimmune encephalomyelitis. *Magn. Reson. Med.* 58:298–305.
- Akbar A, et al. (2008) Increased capsaicin receptor TRPV1-expressing sensory fibres in irritable bowel syndrome and their correlation with abdominal pain. *Gut.* 57:923–9.
- Martelli L, et al. (2007) A potential role for the vanilloid receptor TRPV1 in the therapeutic effect of curcumin in dinitrobenzene sulphonic acid-induced colitis in mice. *Neurogastroenterol. Motil.* 19:668–74.
- Basu S, Srivastava P. (2005) Immunological role of neuronal receptor vanilloid receptor 1 expressed on dendritic cells. *Proc. Natl. Acad. Sci. U. S. A.* 102:5120–5.
- O'Connell PJ, Pingle SC, Ahern GP. (2005) Dendritic cells do not transduce inflammatory stimuli via the capsaicin receptor TRPV1. *FEBS Lett.* 579:5135–9.
- Winer S, et al. (2001) Type I diabetes and multiple sclerosis patients target islet plus central nervous system autoantigens; nonimmunized nonobese diabetic mice can develop autoimmune encephalitis. *J. Immunol.* 166:2831–41.
- Butterfield RJ, et al. (1998) New genetic loci that control susceptibility and symptoms of experimental allergic encephalomyelitis in inbred mice. *J. Immunol.* 161:1860–7.
- Butterfield RJ, et al. (1999) Genetic analysis of disease subtypes and sexual dimorphisms in mouse experimental allergic encephalomyelitis (EAE): relapsing/remitting and monophasic remitting/nonrelapsing EAE are immunogenetically distinct. *J. Immunol.* 162:3096–102.
- Khairatkar-Joshi N, Szallasi A. (2009) TRPV1 antagonists: the challenges for therapeutic targeting. *Trends Mol. Med.* 15:14–22.
- International Multiple Sclerosis Genetics C. (2011) Genome-wide association study of severity in multiple sclerosis. *Genes Immun.* 12:615–25.
- Cunningham S, Patterson CC, McDonnell G, Hawkins S, Vandenbroeck K. (2005) Haplotype analysis of the preprotachykinin-1 (TAC1) gene in multiple sclerosis. *Genes Immun.* 6:265–70.
- Cunningham S, et al. (2007) The neuropeptide genes TAC1, TAC3, TAC4, VIP and PACAP(AD-CYAP1), and susceptibility to multiple sclerosis. *J. Neuroimmunol.* 183:208–13.
- Marrosu MG, et al. (2002) Patients with multiple sclerosis and risk of type 1 diabetes mellitus in Sardinia, Italy: a cohort study. *Lancet.* 359:1461–5.
- Herculano-Houzel S. (2011) Scaling of brain metabolism with a fixed energy budget per neuron: implications for neuronal activity, plasticity and evolution. *PLoS One.* 6:e17514.
- Van Buren JJ, Bhat S, Rotello R, Pauza ME, Premkumar LS. (2005) Sensitization and translocation of TRPV1 by insulin and IGF-I. *Mol. Pain.* 1:17.

51. Sathianathan V, *et al.* (2003) Insulin induces cobalt uptake in a subpopulation of rat cultured primary sensory neurons. *Eur. J. Neurosci.* 18:2477–86.
52. Baker D, *et al.* (2001) Endocannabinoids control spasticity in a multiple sclerosis model. *FASEB J.* 15:300–2.
53. Loria F, *et al.* (2008) Study of the regulation of the endocannabinoid system in a virus model of multiple sclerosis reveals a therapeutic effect of palmitoylethanolamide. *Eur. J. Neurosci.* 28:633–41.
54. Cristino L, *et al.* (2008) Immunohistochemical localization of anabolic and catabolic enzymes for anandamide and other putative endovanilloids in the hippocampus and cerebellar cortex of the mouse brain. *Neuroscience.* 151:955–68.
55. De Petrocellis L, Davis JB, Di Marzo V. (2001) Palmitoylethanolamide enhances anandamide stimulation of human vanilloid VR1 receptors. *FEBS Lett.* 506:253–6.
56. Starowicz K, Cristino L, Di Marzo V. (2008) TRPV1 receptors in the central nervous system: potential for previously unforeseen therapeutic applications. *Curr. Pharm. Des.* 14:42–54.
57. Szallasi A, Cortright DN, Blum CA, Eid SR. (2007) The vanilloid receptor TRPV1:10 years from channel cloning to antagonist proof-of-concept. *Nat. Rev. Drug. Discov.* 6:357–72.
58. Gunthorpe MJ, Chizh BA. (2009) Clinical development of TRPV1 antagonists: targeting a pivotal point in the pain pathway. *Drug Discov. Today.* 14:56–67.